

Institute of Physical Chemistry, Polish Academy of Sciences

ul. Kasprzaka 44/52, 01-224 Warsaw



Volha Vetokhina

**Spectroscopy, photophysics, conformational equilibria,
and photoinduced tautomerization
in selected bifunctional proton donor-acceptor azaaromatic
molecules**

Chapter 7: Supporting Information

B. 444 / 13.201.



Ph.D. dissertation written under the supervision of Prof. dr hab. Jerzy Herbich

Biblioteka Instytutu Chemii Fizycznej PAN

F-B.444/13.zał.



30000000129399

This dissertation has been completed in the framework of the International Ph.D. Studies at the Institute of Physical Chemistry of the Polish Academy of Sciences.

Warsaw 2012

TABLE OF CONTENTS

Table S.3.1	S.4
Scheme S.3.1	S.6
Table S.3.2	S.7
Table S.3.3	S.8
Figure S.3.1	S.9
Figure S.3.2	S.9
Figure S.4.1	S.10
Figure S.4.2	S.14
Figure S.5.1	S.16
Table S.5.1	S.18
Table S.5.2	S.21

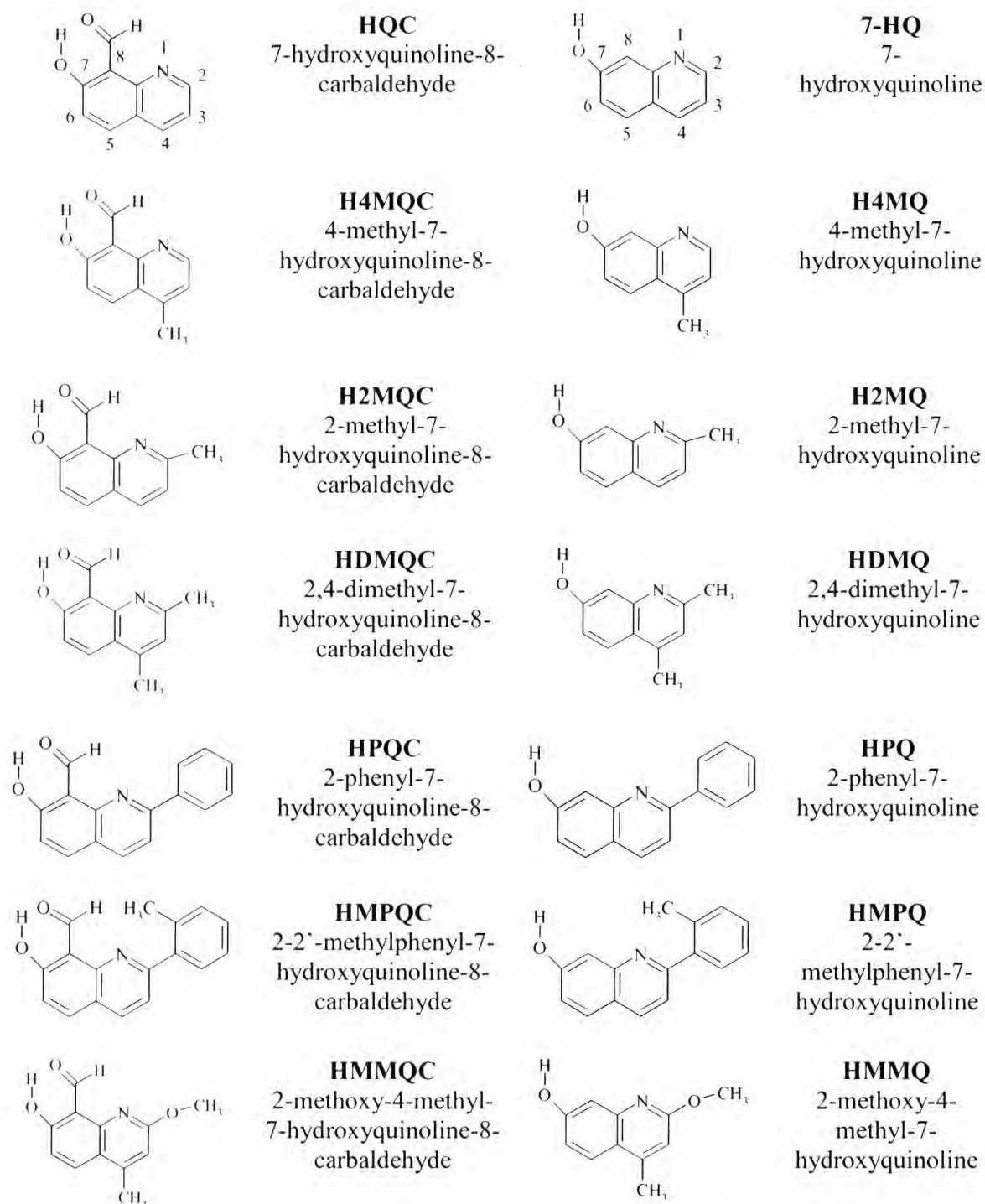
Table S.3.1. Solvent effects on the spectral position of the room temperature fluorescence maxima ($\tilde{\nu}_f$, in cm^{-1}), quantum yields (Φ_f) determined for various excitations (λ_{exc} , in nm), lifetimes (τ , in ns) and resulting radiationless (k_{nr} , in 10^8s^{-1}) and radiative (k_f , in 10^7s^{-1}) rate constants and electronic transition dipole moments corresponding to fluorescence (M_{fl} , in D) of all the **7-HQCs** under study.

Compound	Solvent	λ_{exc}^b	Φ_f^a	$\tilde{\nu}_f^c$	τ^a	k_{nr}	k_f	M_{fl}
HQC	HEX	345	0.005	19500/20500 (NH) ca.24400 (OH)				
	EA	345	0.006	20100(NH); ca.24000 (OH)				
	ACN	356	0.01					
		380	0.04	20200 (NH)				
	1-PrOH	345	0.018	20700 (NH)				
H4MQC	MeOH	343	0.035	20700 (NH)				
	HEX	347	0.002	20700 (NH); 21600 (II); ca.24300 (OH)	6 and < 0.3 < 0.5(d) and 6			
	EA	347	0.003	20600 (NH); ca.24000 (OH)	< 0.5(d) and 6 3(d) and < 0.5			
	ACN	347	0.006	20500 (NH)	≈ 0.7 and 5 < 0.6(d) and 7			
	1-PrOH	345		20900 (NH)				
H2MQC	MeOH	340	0.02	20900 (NH)				
	HEX	346	0.002	19900/20900 (NH) ca.22600 (II) ca.24000 (OH)	< 0.4			
	EA	346	0.005	20900 (NH) ca. 23000	< 0.4			
	ACN	346	0.01					
		380	0.045	20600 (NH)	0.9	10.6	5.0	2.7
1-PrOH	346	0.02	20900 (NH)					
MeOH	380	0.064			0.9	10.4	7.1	3.1
	346			20600 (NH)				
		380						

HDMQC	HEX	348	0.004	21200 (NH) 22300 (II); 23800 (OH)				
	EA	345	0.005	21700				
	ACN	342	0.01					
		370	0.02	21000 (NH)				
	1-PrOH	346	0.023	21400 (NH)				
HMMQC	MeOH	345	0.027	21400 (NH)				
	HEX	346	0.039	21000 (NH)	1.5	6.4	2.6	1.9
	EA	346	0.037	20300 (NH)	1.4	6.9	2.6	2.0
	ACN	346	0.035	19700 (NH)	1.6	6.0	2.2	1.9
	1-PrOH	346	0.04	19700 (NH)	1.8	5.3	2.2	1.9
HPQC	MeOH	346	0.023	19400 (NH)				
	HEX	350	0.003	18100/19200 (NH) <i>ca.</i> 20500 <i>ca.</i> 24000	4.0			
	EA	350	0.005	<i>ca.</i> 20000 (NH) 21500 (II) 23300 (OH)	2.2	5.7(d) and ~0.8		< 0.5(d) and 4.4
	ACN	350	0.013	19600 (NH); 21500 (II) <i>ca.</i> 23500	4.0			< 0.05(d) and 2.7
	1-PrOH	350	0.022	19500 (NH); <i>ca.</i> 22600				3.9(d) and < 0.3
HMPQC	MeOH	350		19100 (NH)				
	HEX	350	0.005	19600 (NH); 23700 (OH)				
	EA	350	0.005					
		372	0.011	19600 (NH), 23700 (OH)				
	ACN	350	0.011					
		393	0.19	19600 (NH)				
	1-PrOH	350	0.03	19600 (NH)				
		376	0.09					
MeOH	350	0.05	19600 (NH)					

^a Error is about 10%. Thus, the maximum error is about 20% for the rate constants k_{nr} and k_f and about 10% for the transition moment M_{if} . ^b Scatter of results: ± 2.0 nm.

^c Scatter of results: ± 150 cm^{-1} , **OH**, **NH**, **II** - assignment of emission. (d) Dominant contribution.



Scheme S.3.1. Formulas, labeling of atoms, acronyms and full names of investigated 7-hydroxyquinoline derivatives.

Table S.3.2. Solvent effects on the spectral position of the room temperature fluorescence maxima ($\tilde{\nu}_f$, in cm^{-1}) corresponding to **OH** (7-quinolinol) and **NH** (7(1H)-quinolinone) tautomeric forms, quantum yields (Φ_f), lifetimes (τ , in ns) and resulting radiationless (k_{nr} , 10^8 in cm^{-1}) and radiative (k_f , 10^8 in cm^{-1}) rate constants and electronic transition dipole moments corresponding to fluorescence (M_f , in D) and the lowest absorption band (M_a , in D) of 7-hydroxyquinolines. λ_{exc} (in nm) – excitation wavelength.

Compound	Solvent	M_a	λ_{exc}	$\tilde{\nu}_f$	Φ_f	τ	k_{nr}	k_f	M_f
HQ*	EA	1.7	320	27900 (OH)	0.06				
	ACN	1.7	320	27600 (OH)	0.08				
	1-PrOH	1.9	330	26500 (OH); 18600 (NH)	0.13				
	MeOH	1.9	330	26300 (OH); 18700 (NH)	0.1				
H4MQ	HEX		335	27200/25800 (OH)					
	EA	1.7	335	27900 (OH)	0.06				
	ACN	1.7	335	27900 (OH)	0.07				
	1-PrOH	1.8	335	26600 (OH); 18900 (NH)	0.15				
	MeOH	1.9	335	26700 (OH); 18800 (NH)	0.13				
H2MQ*	EA	1.9	330	28200 (OH)	0.07	~ 0.7	13	1.0	2.3
	ACN	1.9	330	28200 (OH)	0.07	~ 0.75	12	0.9	2.3
	1-PrOH	2.0	330	26800 (OH)	0.2	2			
				19200 (NH)		5			
	MeOH	2.1	330	26700 (OH); 19200 (NH)	0.16	1.4 4.9			
HDMQ*	EA	2.0	330	28300 (OH)	0.08				
	ACN	2.1	330	28200 (OH)	0.1				
	1-PrOH	2.4	330	26900 (OH); 19200 (NH)	0.23				
	MeOH	2.3	330	27000 (OH); 19400 (NH)	0.21				
HMMQ	HEX		323	30850/30200/29500 (OH)	0.38				
	EA	1.9	323.8	~30300/29250 (OH)	0.42	3.7 (d) and <0.7			
	ACN	1.8	324.5	~30300/29300 (OH)	0.45	4 (d) and 0.9			
	1-PrOH	1.9	325	28500 (OH)	0.38	3 (d) and 1.7			
				20400 (NH)		6.5			
	MeOH	2.0	325	28400 (OH); 20500 (NH)	0.34	2.9 and 1.5 6.1			
HPQ	HEX			28400/27900/27000 (OH)	0.019				
	EA	2.3	340	26400 (OH)	0.14	1.7	4.9	0.8	2.3
	ACN	2.4	340	26200 (OH)	0.16	2	4.2	0.8	2.3
	1-PrOH	2.3	340	25500 (OH)	0.11	3 (d) and < 0.6			
				c.a.17000 (NH)		1 (d) and 6.3			
MeOH	2.5	340	25100 (OH); c.a.17000 (NH)	0.08	2.3(d) and <0.5 1 (d) and 5.1				
HMPQ*	EA	2.1	330	26800 (OH)	0.017				
	ACN	2.0	330	26600 (OH)	0.017				
	1-PrOH	2.6	335	25800 (OH); 17700 (NH)	0.1				
	MeOH	2.1	335	25800 (OH); 17700 (NH)	0.09				

* The solubility in *n*-hexane is too low to measure the absorption and fluorescence spectra

Table S.3.3. Spectral positions of the room temperature absorption (abs) and fluorescence (em) maxima (in cm^{-1}) of **7-HQs** in neutral ACN solutions and under acidic and basic conditions. **C** denotes the assignment of the bands to the tautomeric forms of protonated cations.

	+HClO ₄ <i>c</i> ≅ 3 mol/dm ³		neutral ACN		+NaOH <i>c</i> ≅ 0.2 mol/dm ³	
	abs (C)	em (C)	abs	em	abs	em
7-HQ ^b	28500	22200	30200	27600	-	-
H4MQ ^c	28800	23100	30000	27900	-	-
H2MQ	-	-	30500	28200	-	-
HDMQ ^c	29100	23900	30300	28200	27800	19500
HMMQ	29700	24800	30900	30300/29300	-	-
HPQ	27000	21300	29600	26200	-	-
HMPQ	27600	21900	30200	26600	26800	23300

^a Scatter of results: $\pm 150 \text{ cm}^{-1}$. ^b refs. [S.1, S.2]. ^c our results are similar to those published in ref. [S.2]

[S.1] Mason S. F., Philp J., Smith B. E., *J. Chem. Soc. A*, **1968**, 3051.

[S.2] Senda N., Momotake A., Arai T., *Bull. Chem. Soc. Jpn.*, **2010**, 83, 1272

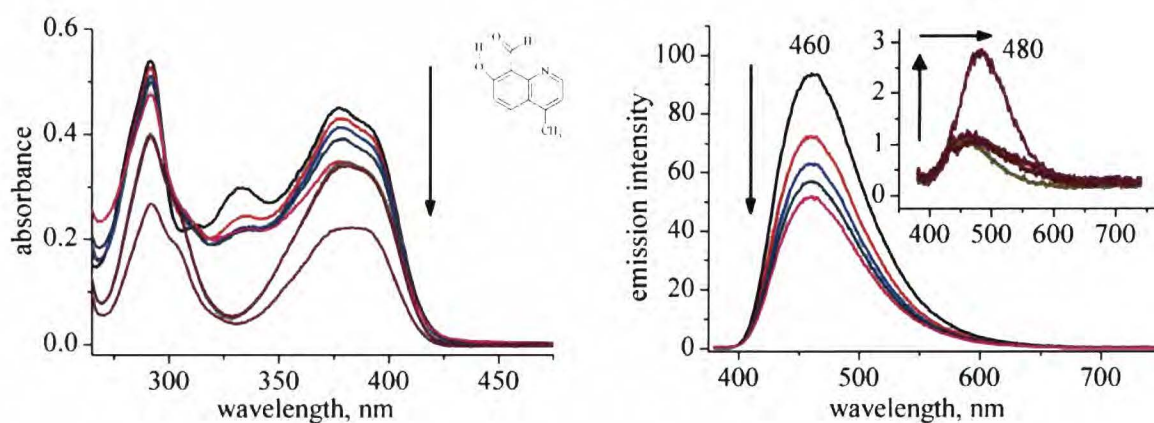


Figure S.3.1. Titration of **H4MQC** solution in water with NaOH at 293 K. Left: changes in absorption; right: evolution of fluorescence bands. The arrows show spectral changes accompanying the addition of NaOH. The sodium hydroxide concentration varied from 0.3 to 8.6 mol/dm³.

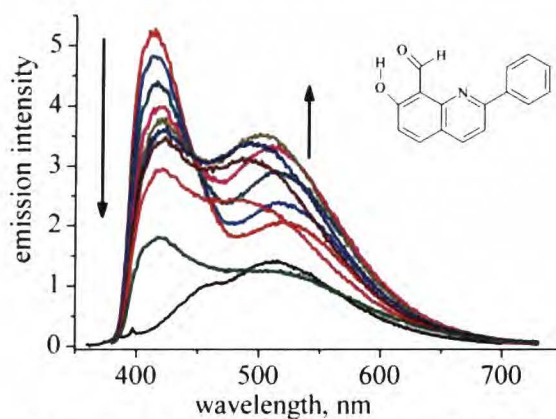
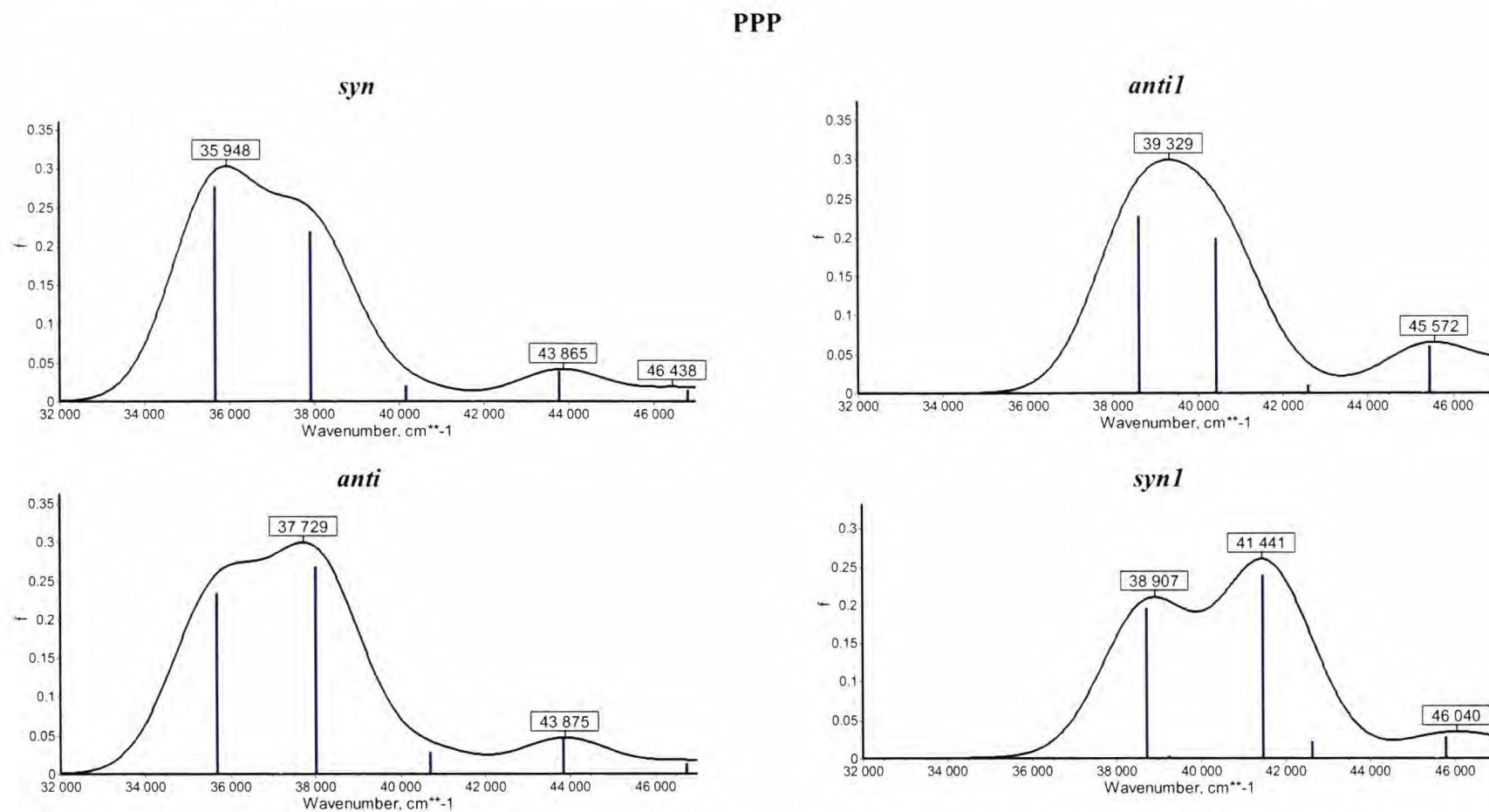
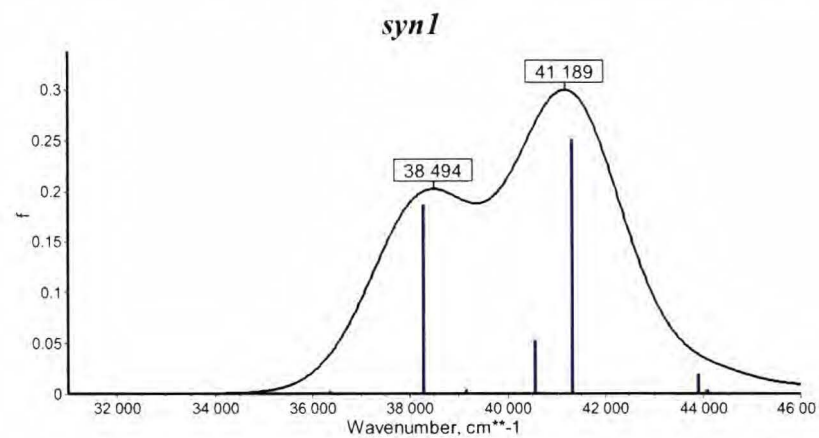
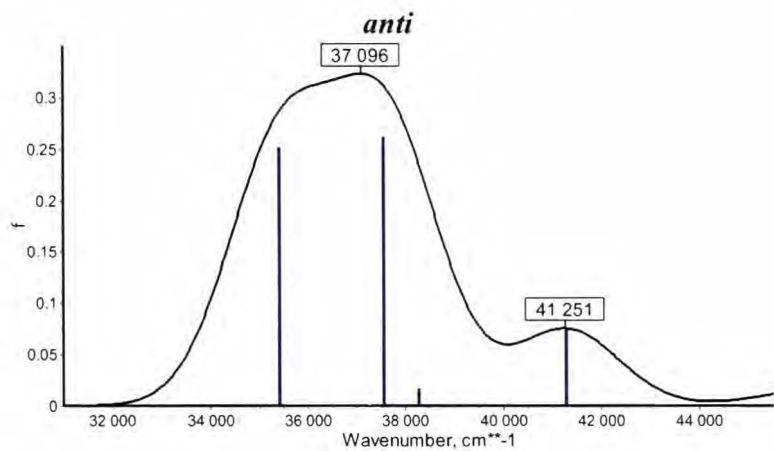
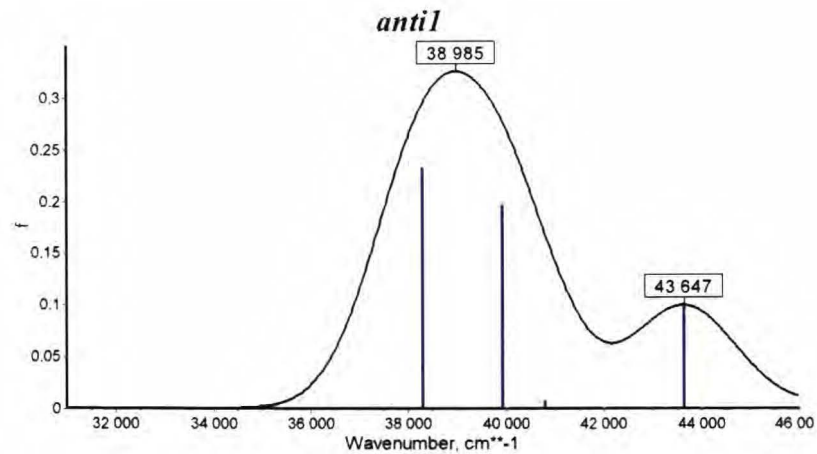
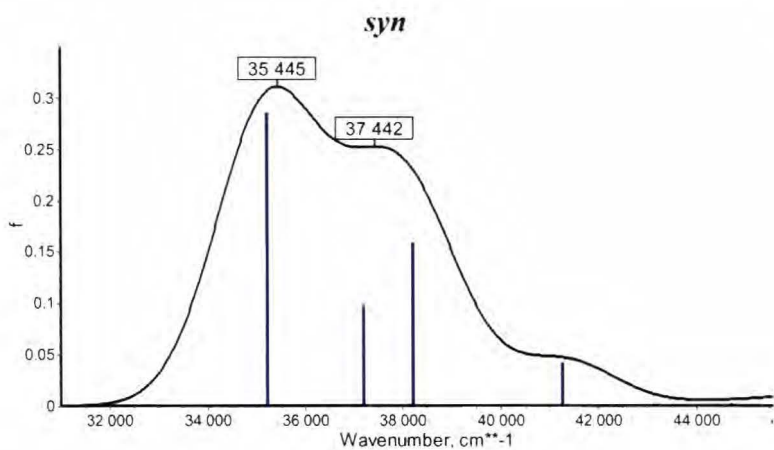


Figure S.3.2. Evolution of fluorescence bands under titration of **HPQC** solution in ACN with 60 % perchloric acid at 293 K. The arrows show spectral changes accompanying the addition of HClO₄. The perchloric acid concentration varied from 0.09 to 4.5 mol/dm³.

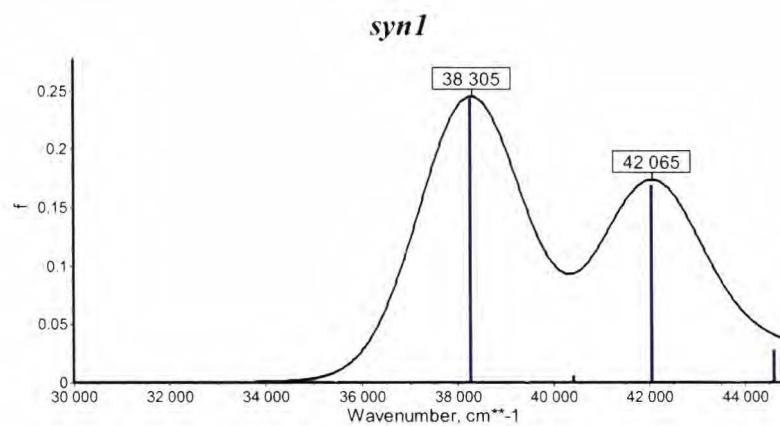
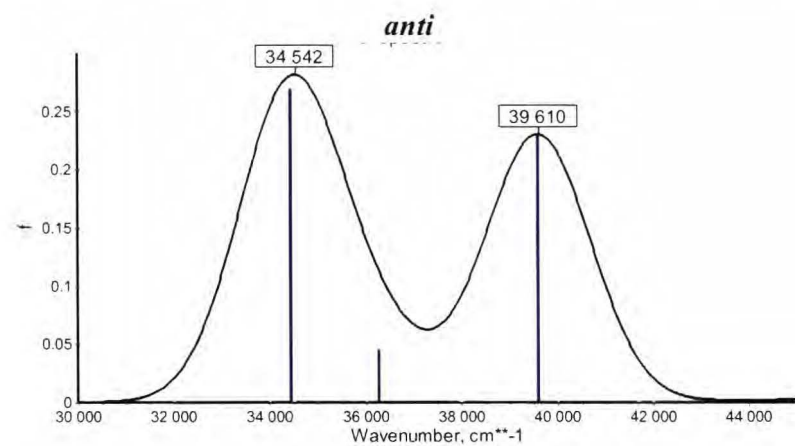
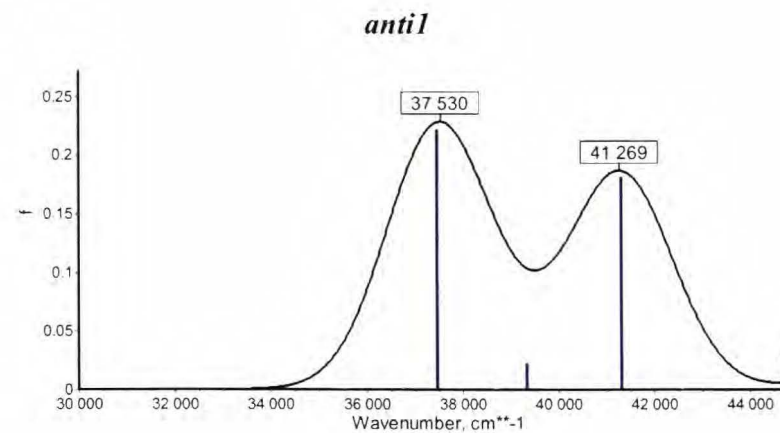
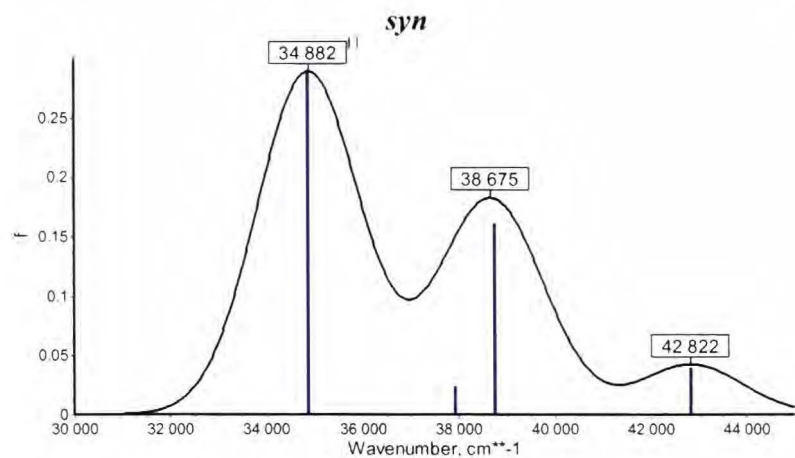
Figure S.4.1. UV-VIS absorption spectra of various rotameric forms of **PPP**, **MPP**, **BPP**, and **NPP** computed at the TD-DFT/B3LYP/6-31+G(d,p) level for the DFT/B3LYP/6-31+G(d,p) ground-state geometry. The spectral envelopes were obtained by convolution of the respective stick spectra with a Gaussian function of 2400 cm^{-1} FWHM.



MPP



BPP



NPP

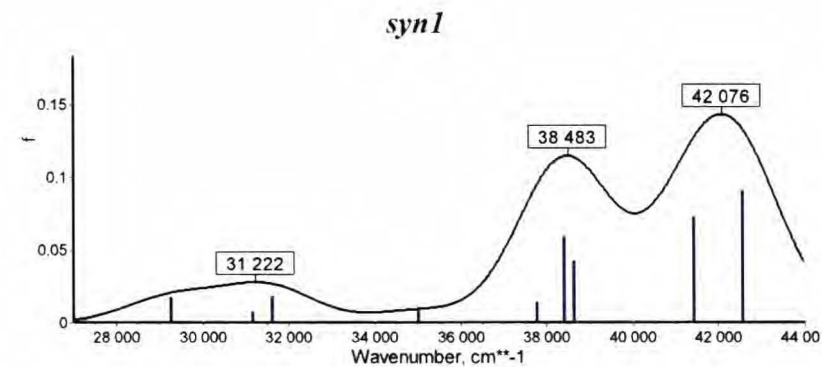
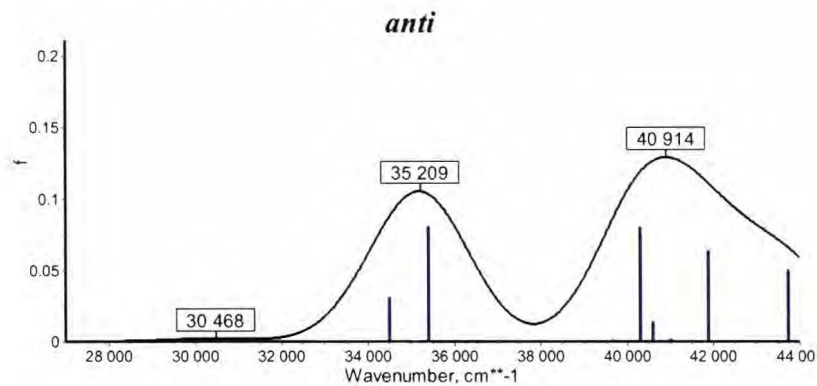
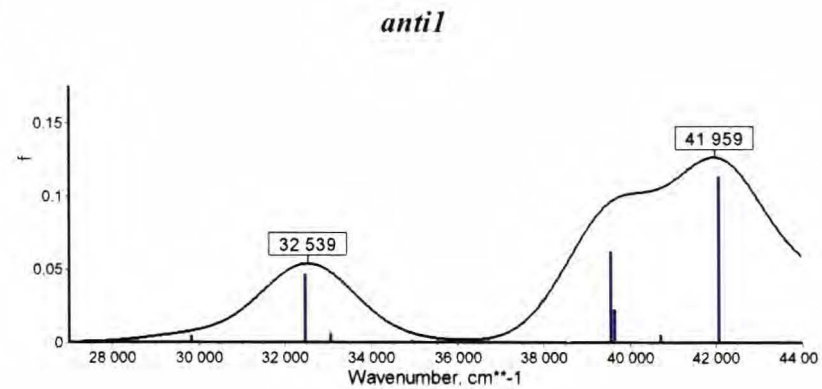
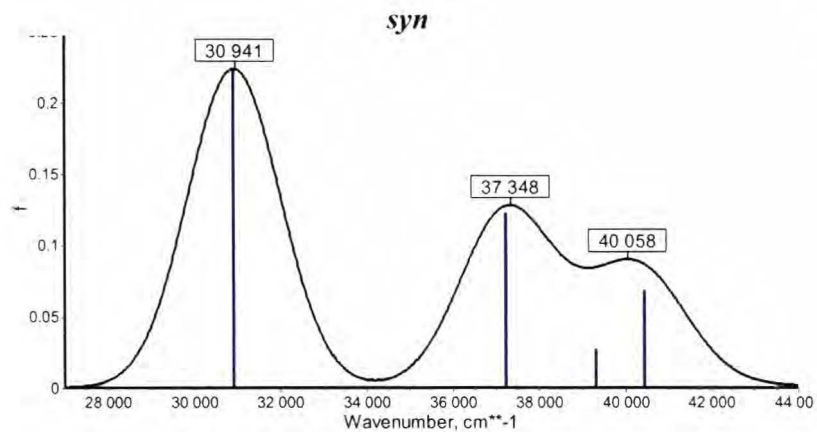
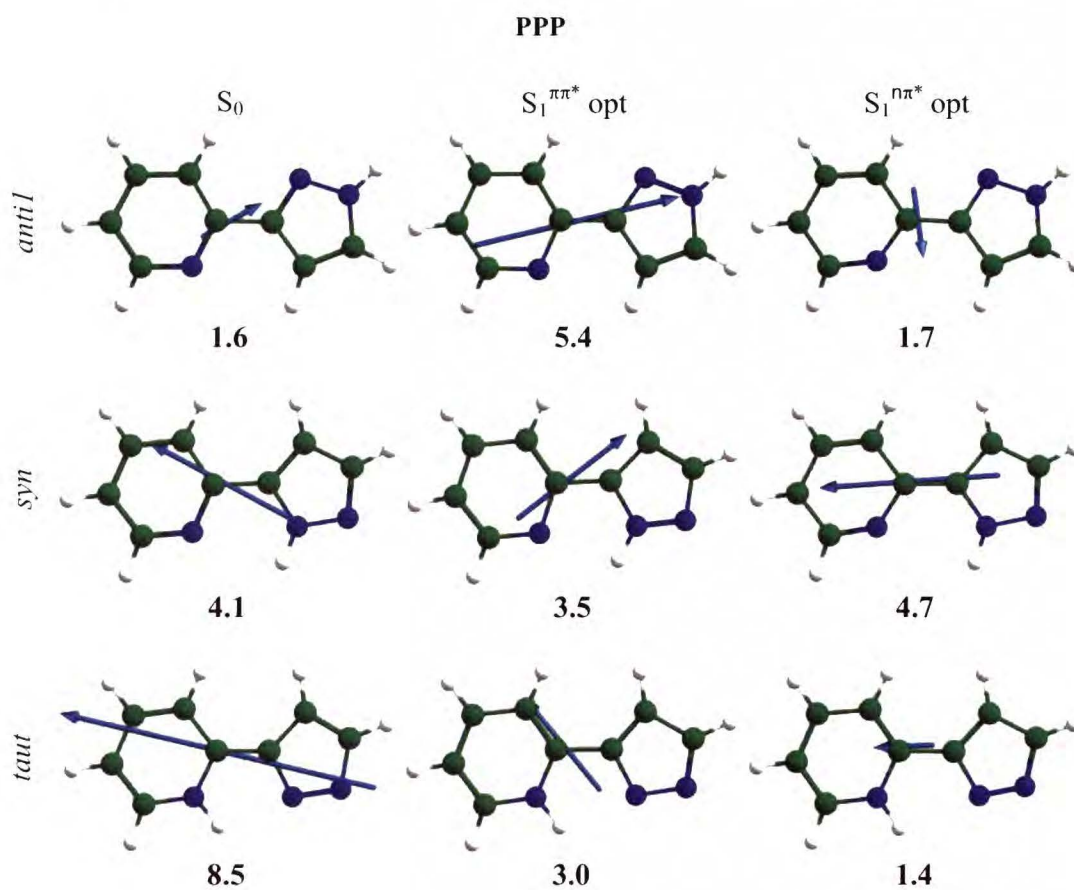


Figure S.4.2. DFT and TD-DFT computed (at the levels of B3LYP/ 6-31+G(d,p)) ground-state and the lowest $^1(\pi, \pi^*)$ excited-state dipole moments of *syn*, *anti*, and *taut* tautomeric/rotameric forms of **PPP**, **MPP**, and **BPP**.



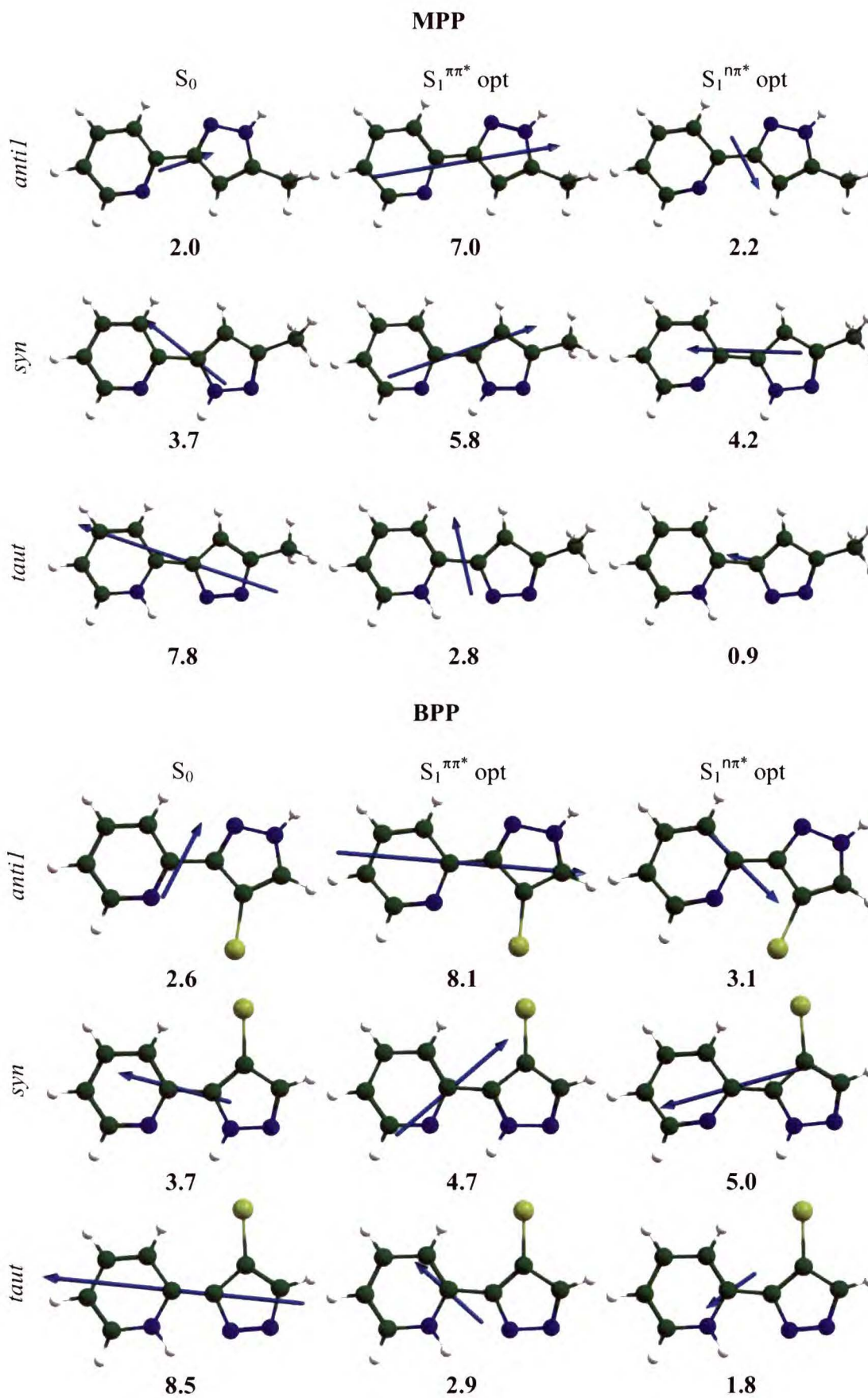
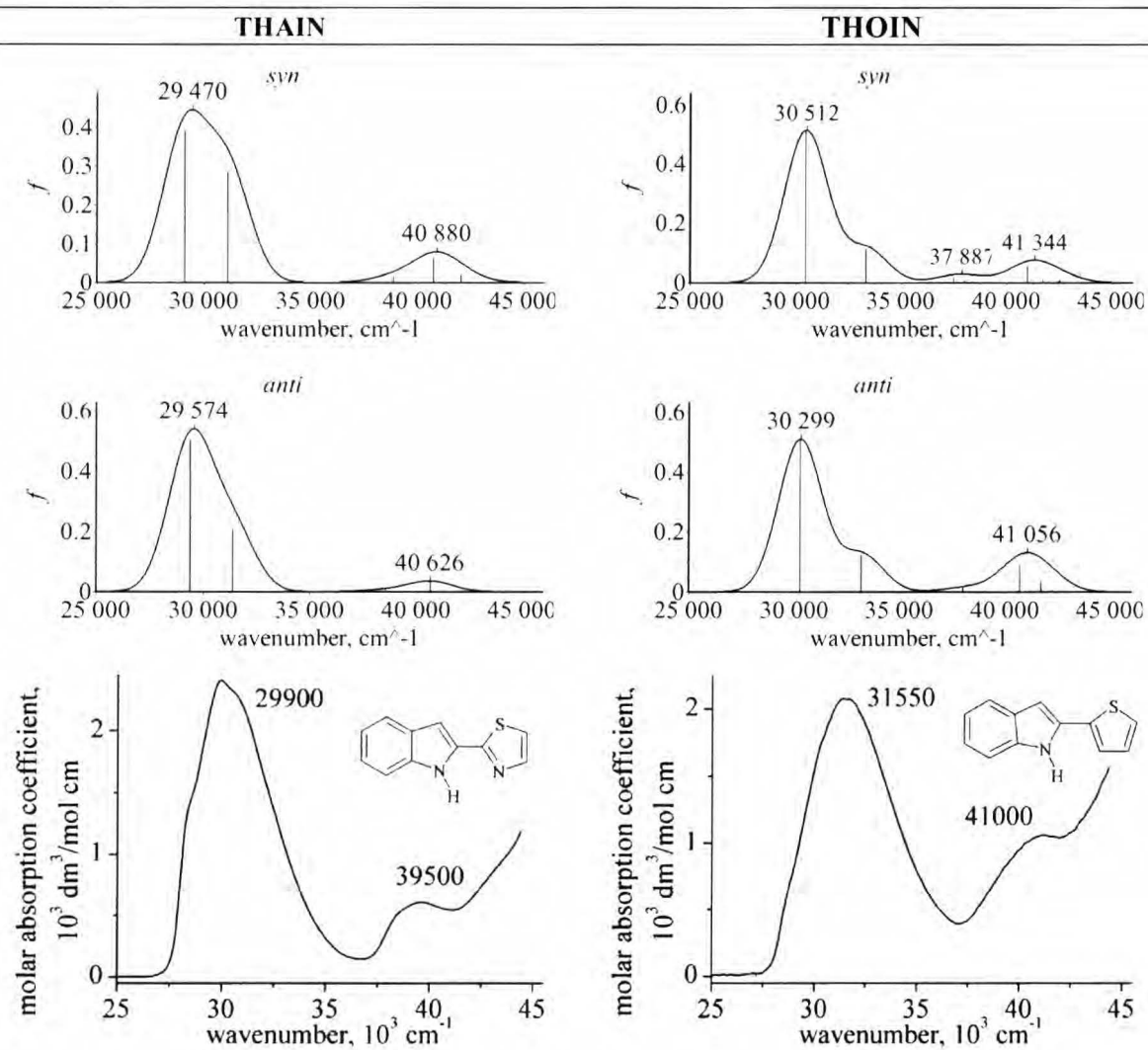


Figure S.5.1. Comparison of the electronic absorption spectra of *syn* (upper) and *anti* (middle) rotameric forms of **THAIN**, **THOIN**, **FURIN**, and **PYRIN** computed at the TD-DFT/B3LYP/6-31+G(d,p) level for the DFT/B3LYP/6-31+G(d,p) geometry (the spectral envelopes are obtained by convolution of the respective stick spectra with a Gaussian function of 2400 cm⁻¹ FWHM) with the spectrum recorded in *n*-hexane (bottom).



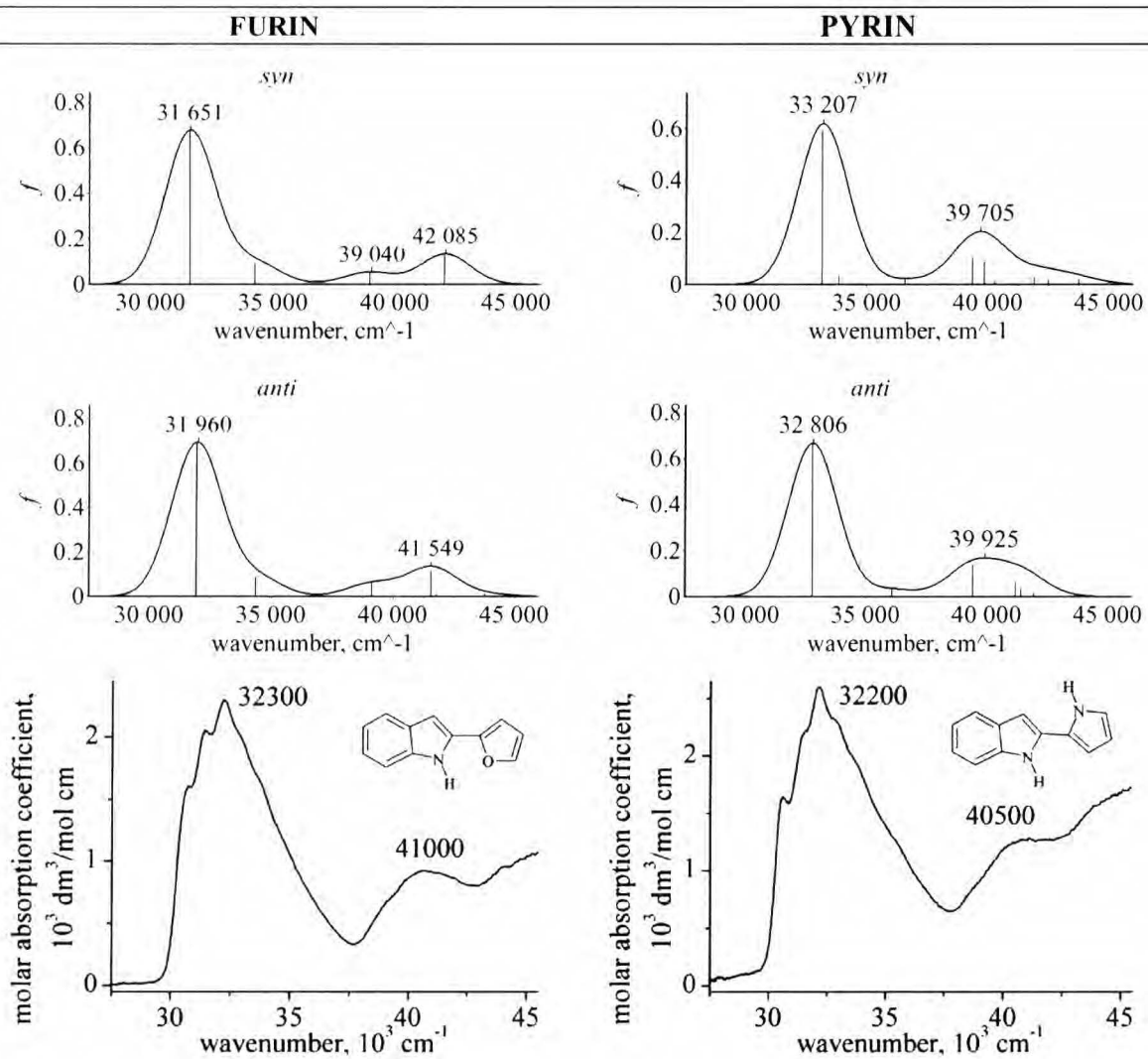
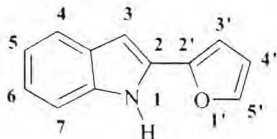


Table S.5.1. Observed (under supersonic jet isolation conditions) and calculated (at DFT, TD-DFT, and CIS B3LYP/6-31+G(d,p) levels) vibrational transitions of **FURIN**. DF – dispersed fluorescence, LIF – laser induced fluorescence excitation, *i* – mode, *sym* – symmetry.

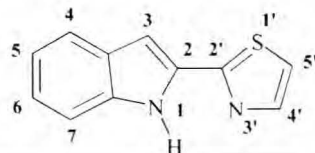


i	sym	Monomer S ₁				LIF	description	Monomer S ₀		DF
		calculations		calculations (DFT)				DF		
		<i>syn</i>	<i>anti</i>	<i>syn</i>	<i>anti</i>					
		ν (DFT)	ν (CIS)	ν (DFT)	ν (CIS)					
63	a'	3532	3609	3540	3582		N-H stretch	3550	3556	
62	a'	3181	3184	3180	3183		furan CH (C5') stretch	3186	3186	
61	a'	3157	3163	3150	3158		furan CH (C3') stretch	3160	3155	
60	a'	3149	3149	3160	3157		C3H stretch	3143	3155	
59	a'	3141	3146	3136	3144		furan CH stretch	3148	3141	
58	a'	3099	3105	3099	3105		benzene CH stretch	3093	3093	
57	a'	3090	3095	3090	3096		benzene CH stretch	3083	3083	
56	a'	3081	3085	3080	3083		benzene CH stretch	3073	3073	
55	a'	3074	3076	3073	3076		benzene CH stretch	3066	3067	
54	a'	1608	1680	1604	1671		C2-C2' stretch, in-plane skeleton deformation	1604	1610	
53	a'	1555	1607	1558	1603		indole in-plane skeleton deformation, CH in-plane bend	1593	1594	
52	a'	1518	1564	1520	1563		indole in-plane skeleton deformation, CH in-plane bend, C2-C2' stretch	1563	1563	
51	a'	1457	1512	1447	1511		furan in-plane skeleton deformation, CH in-plane bend	1519	1513	
50	a'	1444	1508	1445	1503		indole in-plane skeleton deformation, CH, NH in-plane bend	1481	1479	
49	a'	1419	1464	1421	1466		in-plane skeleton deformation, CH, NH in-plane bend	1466	1450	

48	a'	1384	1410	1377	1420	in-plane skeleton deformation, CH, NH in-plane bend	1431	1423
47	a'	1377	1422	1370	1398	in-plane skeleton deformation, furan CH in-plane bend	1398	1405
46	a'	1344	1338	1350	1381	in-plane skeleton deformation, CH, NH in-plane bend	1361	1371
45	a'	1306	1379	1326	1357	in-plane skeleton deformation, CH, NH in-plane bend	1339	1338
44	a'	1289	1317	1275	1311	in-plane skeleton deformation, CH, NH in-plane bend	1313	1318
43	a'	1260	1272	1257	1281	in-plane skeleton deformation, CH, NH in-plane bend	1277	1279
42	a'	1217	1254	1220	1259	NH, C2H in-plane bend, in-plane skeleton deformation	1220	1225
41	a'	1173	1206	1172	1221	in-plane skeleton deformation, CH in-plane bend	1214	1214
40	a'	1162	1216	1158	1200	in-plane skeleton deformation, CH in-plane bend	1199	1203
39	a'	1157	1197	1140	1185	in-plane skeleton deformation, CH in-plane bend	1170	1171
38	a'	1122	1139	1122	1144	benzene CH in-plane bend	1140	1141
37	a'	1110	1152	1104	1142	C5'-O stretch, furan in-plane bend,	1133	1131
36	a'	1070	1107	1071	1104	benzene in-plane CH bend, CC stretch	1099	1098
35	a'	1055	1090	1067	1100	C5'-O stretch, furan, pyrrole CH in-plane bend	1068	1074
34	a'	1018	1045	1017	1048	C5'-O stretch, furan, pyrrole CH in-plane bend	1047	1052
33	a'	986	1006	986	1009	benzene in-plane skeleton deformation	997	998
32	a'	970	1001	981	1002	C2'-O, C5'-O stretch, furan, pyrrole CH in-plane bend	1001	1004
31	a''	915	992	914	993	benzene CH out-of-plane bend	942	942
30	a'	863	885	864	907	in-plane skeleton deformation	871	870
29	a'	856	906	854	882	in-plane skeleton deformation	936	941
28	a'	839	870	838	874	in-plane skeleton deformation	865	867

27	a ^{''}	836	931	834	929		benzene CH out-of-plane bend	903	903	
26	a ^{''}	832	915	824	913		C4'H out-of-plane bend	846	840	
25	a [']	810	831	807	827		in-plane skeleton deformation	863	863	
24	a ^{''}	787	850	789	851		C4H, C7H out-of-plane bend	829	829	
23	a [']	754	769	754	767		in-plane skeleton deformation	771	771	
22	a ^{''}	717	775	737	794		indole out-of-plane skeleton deformation, indole CH out-of-plane bend	773	787	
21	a ^{''}	684	727	676	742		indole out-of-plane skeleton deformation, indole CH out-of-plane bend	739	738	
20	a ^{''}	661	713	692	731		indole CH out-of-plane bend	719	720	
19	a ^{''}	647	742	645	720		C3'H out-of-plane bend	780	765	
18	a ^{''}	624	691	622	707		C5'H out-of-plane bend	700	709	
17	a [']	589	595	588	593		indole in-plane skeleton deformation	596	596	
16	a [']	549	574	550	575		benzene in-plane stretch	571	571	
15	a ^{''}	548	585	585	628		C2-C2' out-of-plane rock	664	672	
14	a ^{''}	533	544	534	549		furan out-of-plane skeleton deformation	579	579	
13	a ^{''}	519	539	521	535		benzene out-of-plane torsion	560	559	
12	a [']	502	522	505	523	512	benzene in-plane skeleton deformation	506	505	
11	a ^{''}	475	475	472	469		NH out-of-plane bend	615	338	
10	a ^{''}	430	293	359	259		NH out-of-plane bend	418	613	
9	a ^{''}	381	407	388	408		C4H, C7H out-of-plane bend	437	432	
8	a [']	322	333	319	337	330	indole in-plane skeleton deformation	327	327	332
7	a [']	299	312	302	315	305	long-axis in-plane stretch	309	306	312
6	a ^{''}	253	252	264	271		indole out-of-plane rock	330	323	
5	a ^{''}	217	226	219	228		indole out-of-plane torsion	236	236	
4	a ^{''}	150	152	158	167		out-of-plane rock	195	193	
3	a [']	89	94	96	98	89	C2-C2' in-plane rock	101	103	105
2	a ^{''}	89	98	77	83		C2-C2' out-of-plane torsion	46	31	
1	a ^{''}	57	50	58	56		C2-C2' out-of-plane rock	68	68	

Table S.5.2. Observed (under supersonic jet isolation conditions) and calculated (at DFT, TD-DFT, and CIS B3LYP/6-31+G(d,p) levels) vibrational transitions of **THAIN**. DF – dispersed fluorescence, LIF – laser induced fluorescence excitation, *i* – mode, *sym* – symmetry.



i	sym	Monomer S ₁ calculations				LIF <i>v</i>	Description	Monomer S ₀ calculations (DFT)		DF
		<i>syn</i>		<i>anti</i>				<i>syn</i>	<i>anti</i>	
		<i>v</i> (DFT)	<i>v</i> (CIS)	<i>v</i> (DFT)	<i>v</i> (CIS)					
60	a'	3495	3594	3514	3598		NH stretch	3535	3543	
59	a'	3159	3160	3157	3160		C5'H stretch	3162	3163	
58	a'	3150	3145	3168	3170		C3H stretch	3140	3161	
57	a'	3104	3107	3103	3114		benzene CH stretch	3094	3095	
56	a'	3100	3116	3100	3106		C4'H stretch	3119	3128	
55	a'	3093	3099	3093	3097		benzene CH stretch	3084	3084	
54	a'	3085	3088	3083	3086		benzene CH stretch	3076	3075	
53	a'	3080	3080	3078	3078		benzene CH stretch	3068	3069	
52	a'	1583	1651	1585	1644		indole CH in-plane bend, skeleton deformation	1604	1604	
51	a'	1553	1617	1547	1616		C2-C2' stretch, CH in-plane bend, skeleton deformation	1568	1567	
50	a'	1518	1581	1503	1575		C2-C2' stretch, CH in-plane bend, skeleton deformation	1543	1534	
49	a'	1438	1515	1442	1515		CH in-plane bend, skeleton deformation	1480	1484	
48	a'	1418	1466	1412	1465		CH in-plane bend, skeleton deformation	1468	1476	
47	a'	1388	1446	1400	1447		CH, N1H in-plane bend, skeleton deformation	1432	1433	
46	a'	1384	1397	1369	1405		C4'H in-plane bend, C5'-C4', C4'-N3' stretch	1406	1418	
45	a'	1329	1385	1339	1383		CH in-plane bend, skeleton deformation	1395	1396	
44	a'	1324	1367	1324	1376		CH, N1H in-plane bend, skeleton deformation	1346	1338	
43	a'	1316	1340	1308	1320		CH, N1H in-plane bend, skeleton deformation	1326	1316	
42	a'	1277	1262	1280	1284		CH, N1H in-plane bend, skeleton deformation	1299	1297	

41	a'	1243	1289	1251	1266		CH, N1H in-plane bend, skeleton deformation	1282	1275	
40	a'	1217	1246	1213	1248		CH, N1H in-plane bend, skeleton deformation	1213	1219	
39	a'	1175	1212	1168	1207		CH, N1H in-plane bend, skeleton deformation	1204	1212	
38	a'	1152	1205	1160	1193		CH, N1H in-plane bend, skeleton deformation	1172	1163	
37	a'	1127	1140	1127	1149		C5H, C6H in-plane bend	1137	1134	
36	a'	1087	1133	1094	1133		C2'-S1', C2'-N3' in-plane stretch, C3H bend	1120	1124	
35	a'	1063	1108	1066	1098		indole in-plane skeleton deformation	1100	1100	
34	a'	1037	1064	1040	1072		C5'H in-plane bend	1050	1046	
33	a'	1003	1010	963	992		in-plane skeleton deformation	1027	1012	
32	a'	983	1002	993	1006		in-plane skeleton deformation	996	996	
31	a''	927	1002	927	1002		benzene out-of-plane CH bend	945	946	
30	a''	878	956	871	953		benzene out-of-plane CH bend	909	908	
29	a'	863	887	863	881		in-plane skeleton deformation	871	871	
28	a'	849	895	848	891		in-plane skeleton deformation	890	882	
27	a''	837	942	850	948		C4'H out-of-plane bend	867	870	
26	a'	835	865	822	855		in-plane skeleton deformation	848	845	
25	a''	825	861	819	865		benzene out-of-plane CH bend	831	803	
24	a'	760	776	760	776		in-plane skeleton deformation	771	772	
23	a''	724	783	739	811		indole out-of-plane skeleton deformation, indole CH out-of-plane bend	781	833	
22	a'	697	730	682	719		in-plane skeleton deformation	725	721	
21	a''	695	721	692	729		indole out-of-plane skeleton deformation, indole CH out-of-plane bend	740	740	
20	a''	684	735	701	748		indole CH out-of-plane bend	721	723	
19	a'	606	623	596	622	596	in-plane skeleton deformation	627	620	
18	a''	603	620	594	637		C2-C2' out-of-plane rock, C3H out-of-plane bend	656	645	
17	a'	581	595	580	592	571	indole in-plane skeleton deformation	595	594	609
16	a''	575	660	583	663		C5'H out-of-plane bend	693	687	
15	a''	566	412	460	247		N1H out-of-plane bend	472	331	
14	a'	536	560	538	558		benzene in-plane stretch	560	560	564
13	a''	530	553	522	558		out-of-plane skeleton deformation	597	593	

12	a ^{''}	520	540	531	543		out-of-plane skeleton deformation	560	558	
11	a [']	470	488	465	489	485	benzene in-plane skeleton deformaton	477	469	461
10	a ^{''}	389	446	391	443		C4H, C7H out-of-plane bend	428	427	
9	a ^{''}	324	359	334	381		thiazole out-of-plane rock	506	496	
8	a [']	308	318	308	319	307	indole in-plane skeleton deformation	317	314	
7	a ^{''}	286	262	278	270		out-of-plane rock	314	313	
6	a [']	259	270	254	270	263	long-axis in-plane stretch	262	267	270
5	a ^{''}	222	232	212	234		indole out-of-plane torsion	240	237	
4	a ^{''}	137	141	131	136		out-of-plane rock	189	186	
3	a [']	80	88	90	93	78	C2-C2' in-plane rock	96	96	94
2	a ^{''}	72	87	43	68		C2-C2' out-of-plane torsion	48	14	
1	a ^{''}	48	50	49	46		C2-C2' out-of-plane rock	66	66	



B
444/13.201

F-B.444/13.zał.



30000000129399